

# Properties of Al/Al<sub>2</sub>O<sub>3</sub>-TiO<sub>2</sub> composites prepared by powder metallurgy processing

H. Aydın\*, P. C. Tokat Birgin

<sup>1</sup>Department of Metallurgy and Material Engineering, Kütahya Dumlupınar University, 43100 Kütahya, Turkey

Received 11 November 2020, received in revised form 25 March 2021, accepted 12 April 2021

## Abstract

In this paper, aluminum metal matrix composite (AMC<sub>s</sub>) containing Al<sub>2</sub>O<sub>3</sub>-TiO<sub>2</sub> composite powder in different ratios (5, 10, 15, and 20 wt.%) as a reinforcement material was produced using the powder metallurgy method. This paper aims to research the effect of the alumina-titanium oxide powder ratio on Al/Al<sub>2</sub>O<sub>3</sub>-TiO<sub>2</sub> composite properties. An experimental study has been carried out on density, hardness, tensile strength, phase, and microstructure characterization of aluminum metal matrix composites. The findings of the experimental investigation reveal that the AMC<sub>s</sub> with 20 wt.% Al<sub>2</sub>O<sub>3</sub>-TiO<sub>2</sub> exhibited gradually increased mechanical properties, i.e., Vickers hardness of 56 HV and the tensile strength of 150 MPa. It has been concluded that the density of composites improved with the addition of Al<sub>2</sub>O<sub>3</sub>-TiO<sub>2</sub> reinforcement. Microstructural observation indicates that the distribution of Al<sub>2</sub>O<sub>3</sub>-TiO<sub>2</sub> particles is usually near-uniform and homogeneous in the aluminum matrix.

**Key words:** aluminum-based composite, powder metallurgy, Al/Al<sub>2</sub>O<sub>3</sub>-TiO<sub>2</sub>, mechanical behavior

## 1. Introduction

Similar to polymer and ceramic matrix composites, metal matrix composites (MMC<sub>s</sub>) take advantage of strong, stiff but brittle reinforcements to improve composite strength and stiffness. The improved properties of metal matrix composites make them an effective alternative to traditional engineering materials. MMC<sub>s</sub> are comprised of titanium, aluminum, magnesium, copper, and their alloys as a matrix along with a typical reinforcement ceramic material such as carbide, oxide, and boride, in the form of fiber or particles [1]. Particle-reinforced metal matrix composites have paved the way for a unique field of materials science and engineering over the past decade as potential applications for aerospace, automotive, and other structural components. The ceramic reinforcement phase is frequently used in metal matrix composites for improving their mechanical and thermal properties.

Aluminum matrix composites have attracted the attention of materials scientists because of the magnificent combination of properties (such as high strength, low density, improved wear resistance, and ther-

mal properties). Hence, fields such as automotive, aerospace, gas turbine engines, helicopters, military aircraft, etc., have used these materials as lightweight components [2].

Aluminum matrix composites have been under development for many years, with many different types of reinforcement attempted with varying degrees of success. Continuous and short fibers, whiskers, and particulates can be considered among these. Ceramic particle reinforced composites display enhanced strength due to dislocation and dispersion strengthening. Moreover, ceramic particles also provide support for improving the hardness of MMC<sub>s</sub> [3]. TiB<sub>2</sub>, ZrB<sub>2</sub>, TiC, SiC, Al<sub>2</sub>O<sub>3</sub>, and B<sub>4</sub>C can be indicated as commonly used ceramic reinforced phases for aluminum matrix composites (AMMC<sub>s</sub>). Aluminum oxide (Al<sub>2</sub>O<sub>3</sub>) and titanium oxide (TiO<sub>2</sub>) make up a primarily inherent reinforcement material for aluminum matrix composites since they effectively combine physical and mechanical properties such as high melting point, high hardness, low density, high elastic modulus, and outstanding wear resistance [4–7].

Many processing methods have been developed

\*Corresponding author: e-mail address: [hedive.avdin@dpu.edu.tr](mailto:hedive.avdin@dpu.edu.tr)

Table 1. Composition of Al and Al<sub>2</sub>O<sub>3</sub>-TiO<sub>2</sub> powder from XRF data (wt.%)

Aluminum powder	Al	C	Fe	Si	Cu	S	Co	Zn	Mn	Loss of temp.
	99.99	–	0.01	–	–	–	–	–	–	–
Al <sub>2</sub> O <sub>3</sub> -TiO <sub>2</sub> powder	Na <sub>2</sub> O	MgO	Al <sub>2</sub> O <sub>3</sub>	SiO <sub>2</sub>	SO <sub>3</sub>	K <sub>2</sub> O	TiO <sub>2</sub>	Fe <sub>2</sub> O <sub>3</sub>	ZrO <sub>2</sub>	Loss of temp.
	0.27	0.08	84.00	0.21	0.05	0.02	14.15	0.20	0.46	0.38

for Al metal matrix composites. Previous works have focused primarily on Al metal matrix composites (AMMC<sub>s</sub>) fabricated by stirring casting [8, 9], melt infiltration [10], powder metallurgy [11, 12], and spray deposition [12, 13]. Uniform distribution of reinforcement particles in the matrix, higher mechanical properties, minimum undesirable interfacial reactions, and the low-cost processing method can be attained through powder metallurgy (PM) [11]. The PM approach has the benefit of reducing the interaction among the ceramic reinforcement and the matrix through semisolid and/or solid-state processing. It also has various other advantages: its capacity to combine various matrix reinforcements in the same composite and achieve high reinforcement volume fractions [14].

PM was used in the present study to synthesize Al metal matrix composite (AMMC<sub>s</sub>) using Al<sub>2</sub>O<sub>3</sub>-TiO<sub>2</sub> reinforcement, after which the impacts of the Al<sub>2</sub>O<sub>3</sub>-TiO<sub>2</sub> content on structural and mechanical properties were examined. The objective of the present study was to establish a basis for the processing of high-performance AMMC<sub>s</sub> reinforced by ceramic particles using powder metallurgy.

## 2. Experimental

Aluminum (Al) with a particle size smaller than 40 μm (99.99% purity, Acros Organics) and Al<sub>2</sub>O<sub>3</sub>-TiO<sub>2</sub> composite powder with a particle size of 30.6 μm (99.99% purity, Metco) were used in the study as starting materials. The powders of aluminum (Al) and alumina-titanium oxide (Al<sub>2</sub>O<sub>3</sub>-TiO<sub>2</sub>) were first characterized for compositions using wavelength dispersive X-ray fluorescence (XRF) (Panalytical/Axios MAX), the results of which are presented in Table 1. Composite samples were produced with different weight contents of Al<sub>2</sub>O<sub>3</sub>-TiO<sub>2</sub>: 5, 10, 15, and 20 wt.%. Required amounts of Al and Al<sub>2</sub>O<sub>3</sub>-TiO<sub>2</sub> powders were mixed and ball milled for 1 h in alumina pot using alumina ball as grinding media at the speed of 300 rpm min<sup>-1</sup> to achieve a specific weight content of a composite sample. During the mixing process, ~ 35 wt.% ethanol was added to decrease the possibility of agglomerate formation. The dried powder was pressed in a die under a pressure of 2 tons

for preparing the pellets. The pressed samples were sintered further in a tube furnace at 800 °C in an argon atmosphere. The samples were heated from room temperature up to 800 °C at a rate of 5 °C min<sup>-1</sup>, then sintered at that temperature for 4 h, and cooled back naturally to room temperature.

Archimedes' method was used for determining the density of sintered composites. Phase characterization was performed via X-ray diffraction (XRD) using a Panalytical, empyrean brand model X-ray diffractometer with a Cu Kα radiation source operating at 40 kV and 40 mA. The microstructures and phase compositions were examined via scanning electron microscopy (SEM) and energy-dispersive X-ray spectroscopy (EDS) (FEI Nova NanoSEM 650). Vickers hardness experiments were performed to determine the hardness of the sintered samples. Sintered pure Al and composite samples were placed inside a mold with epoxy resin and sanded with SiC paper. They were polished with a diamond paste to obtain a correct measurement of the indentation length created before the hardness test. The tensile properties of the composites at room temperature were determined using an Instron material-testing machine (INSTRON, 50 kN) at a cross-head speed of 0.5 mm s<sup>-1</sup>. The ultimate tensile strength of the sample was calculated using three bars test samples 75 mm × 5 mm × 55 mm in size.

## 3. Results and discussion

### 3.1. Structural analysis

The aluminum powder used has high purity as shown by X-ray fluorescence (XRF) data (Table 1) and X-ray diffraction (XRD) peak (Fig. 1) exhibited at 2θ values of 38.3°, 44.7°, 65.0°, and 78.1° corresponding to *d*<sub>111</sub>, *d*<sub>200</sub>, *d*<sub>220</sub>, and *d*<sub>311</sub> planes of aluminum, respectively. Figure 1 shows no peak from other elements, which shows the purity of aluminum and alumina-titanium oxide powder. XRD of alumina displayed peaks at 2θ angles of 25.6°, 36.2°, 43.2°, 52.5°, 57.4°, 66.2°, and 68.1°. XRD of titanium oxide depicted peaks at 2θ angles of 25.4°, 37.6°, 49.3°, 53.6°, 54.5°, 59.6°, 62.4°, 63.4°, and 65.9°.

XRD spectra illustrate that the peak intensity

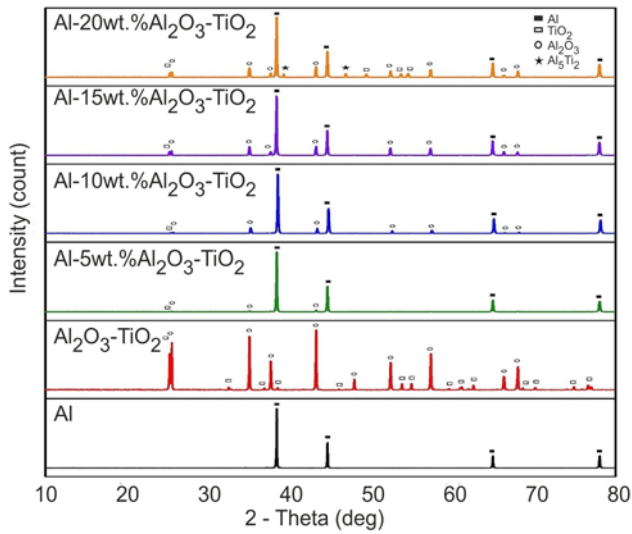


Fig. 1. XRD analysis of Al metallic powder, alumina-titanium oxide ( $\text{Al}_2\text{O}_3\text{-TiO}_2$ ) powder, 5 %  $\text{Al}/\text{Al}_2\text{O}_3\text{-TiO}_2$ , 10 %  $\text{Al}/\text{Al}_2\text{O}_3\text{-TiO}_2$ , 15 %  $\text{Al}/\text{Al}_2\text{O}_3\text{-TiO}_2$ , and 20 %  $\text{Al}/\text{Al}_2\text{O}_3\text{-TiO}_2$  composites.

corresponding to aluminum (Al) decreases while the corresponding intensities of the peak associated with  $\text{Al}_2\text{O}_3$  and  $\text{TiO}_2$  increase slightly with the decrease of the weight fraction of aluminum. XRD of alumina depicted major peaks at  $2\theta$  angles of  $25.6^\circ$ ,  $36.2^\circ$ ,  $43.2^\circ$ , and  $57.4^\circ$ . JCPDS card no. of this phase is 98-0006-5594. Alumina phase has been observed in similar studies in the literature involving  $\text{Al}/\text{Al}_2\text{O}_3$  [15]. XRD of titanium oxide depicted major peaks at  $2\theta$  angles of  $25.4^\circ$ ,  $53.6^\circ$ , and  $54.5^\circ$ . The experimental XRD pattern is in accordance with the JCPDS card no. 98-000-9852 (Anatase,  $\text{TiO}_2$ ) and the  $2\theta$  at peak  $25.4^\circ$  affirms the  $\text{TiO}_2$  anatase structure [14]. XRD of the compound containing aluminum titanium intermediate phase ( $\text{Al}_5\text{Ti}_2$ ) depicted major peaks at  $2\theta$  angles of  $39.2^\circ$  and  $46.8^\circ$ . JCPDS card no. of this phase is 98-010-6255. It is observed in studies involving  $\text{Al}/\text{Al}_2\text{O}_3\text{-TiO}_2$  in the literature that intermediate phases containing aluminum titanium have been formed [16].

In our work, after the treatment of the sample at  $800^\circ\text{C}$ , growth mechanism of the intermetallic zone in  $\text{Al-TiO}_2$  liquid-solid interface changes following the

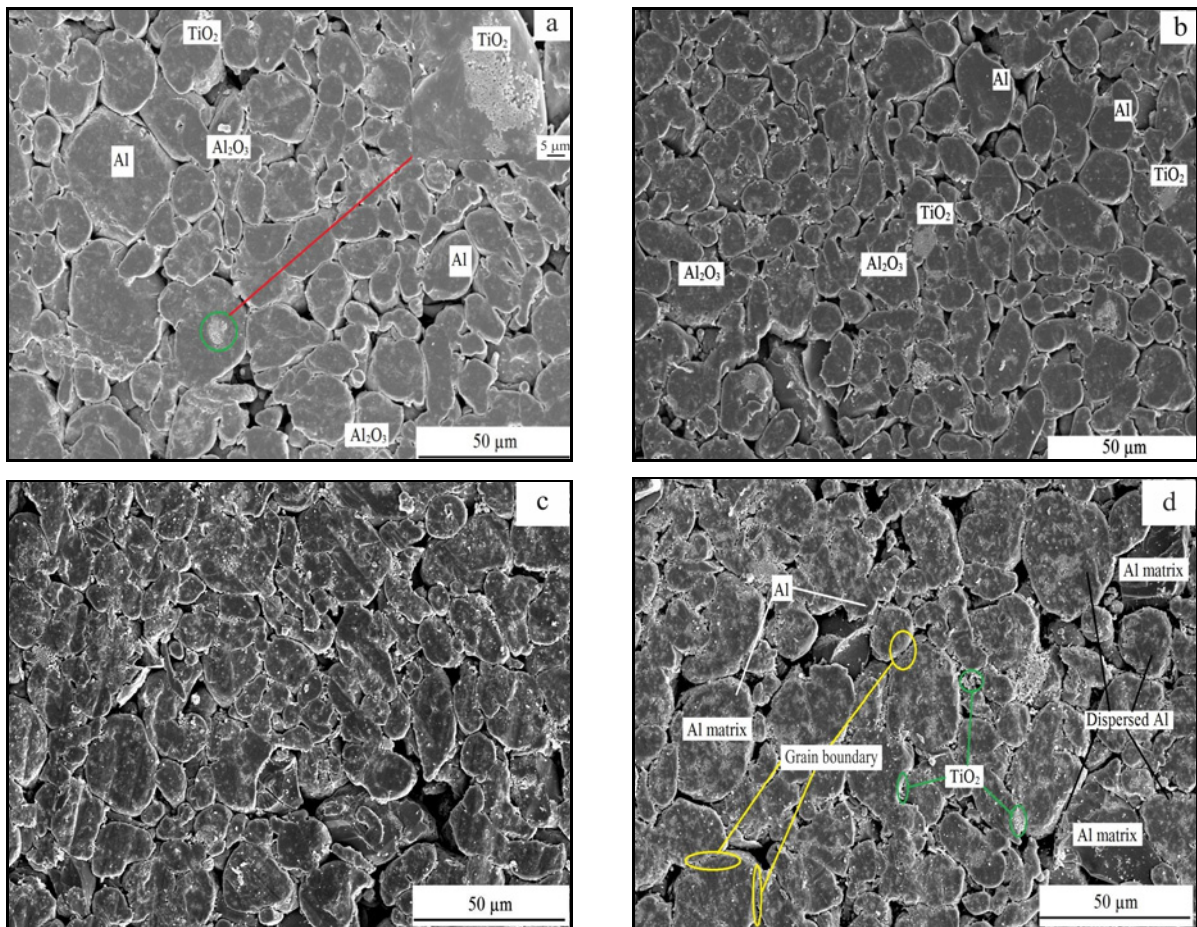


Fig. 2. SEM images of composite samples of Al-5 wt.%  $\text{Al}_2\text{O}_3\text{-TiO}_2$  (a), Al-10 wt.%  $\text{Al}_2\text{O}_3\text{-TiO}_2$  (b), Al-15 wt.%  $\text{Al}_2\text{O}_3\text{-TiO}_2$  (c), and Al-20 wt.%  $\text{Al}_2\text{O}_3\text{-TiO}_2$  (d).

phase transition of Ti, from being dominated by the dissolution rate of  $\text{TiO}_2$  in molten Al to that by the chemical reaction speed of the atoms of Al and Ti. It has been proven that among all Ti-Al compounds,  $\text{Al}_3\text{Ti}$ , Al-Ti, and  $\text{AlTi}_3$  can be directly formed by the reaction between Ti and Al, while  $\text{Al}_2\text{Ti}$  and  $\text{Al}_5\text{Ti}_2$  can be formed only through a series of intermediate reactions [15]. Researchers investigated the phase diagram of the Al-Ti-O system. Among all the reported isothermal sections of the Ti-Al-O system, reported phase diagram evaluations (isothermal sections) have usually been carried out at 945, 900, 871, 800, 700, and 500°C [17–20]. Usually, ceramic particles are difficult to react with molten Al. Maity et al. [15] reported that though the reactive oxide particles' wettability should be better, up to only 3 wt.%  $\text{TiO}_2$  and 20 vol.%  $\text{Al}_2\text{O}_3$  could be incorporated into the molten Al. When we look at stoichiometry, approximately the same amounts of  $\text{TiO}_2$  and  $\text{Al}_2\text{O}_3$  were used in our study.

SEM images of composite samples of Al/ $\text{Al}_2\text{O}_3$ - $\text{TiO}_2$  at different compositions display the varying weight percentage of  $\text{Al}_2\text{O}_3$ - $\text{TiO}_2$  particles (Fig. 2).

The presence of ceramic particles inside the aluminum metal matrix is proven with the micro-level examination. The microstructure of all composites consists of rounded  $\text{Al}_2\text{O}_3$  and  $\text{TiO}_2$  grains, scattered both intra-granularly and intergranularly. Intergranular  $\text{Al}_2\text{O}_3$  and  $\text{TiO}_2$  grains also appeared as agglomerates with pores between them.

Figure 2 displays the even distribution of reinforcing particles ( $\text{Al}_2\text{O}_3$  and  $\text{TiO}_2$ ) within the Al matrix, which was discerned using a scanning electron microscope when the weight percentage of the particles increased in Al/ $\text{Al}_2\text{O}_3$ - $\text{TiO}_2$ . It is apparent that some visible clusters are found. Moreover, particle distribution is found to be almost homogeneous. As mentioned in similar previous works by the authors, the formation of agglomeration can be ascribed to the mixing conditions and/or sintering process [14, 22]. Kang and Chan [21] put forth that agglomeration can contribute to the composites' strengthening if the agglomeration appears to be well bonded to the matrix.

The weight percentage and distribution of ceramic reinforcement in the metallic matrix signifi-

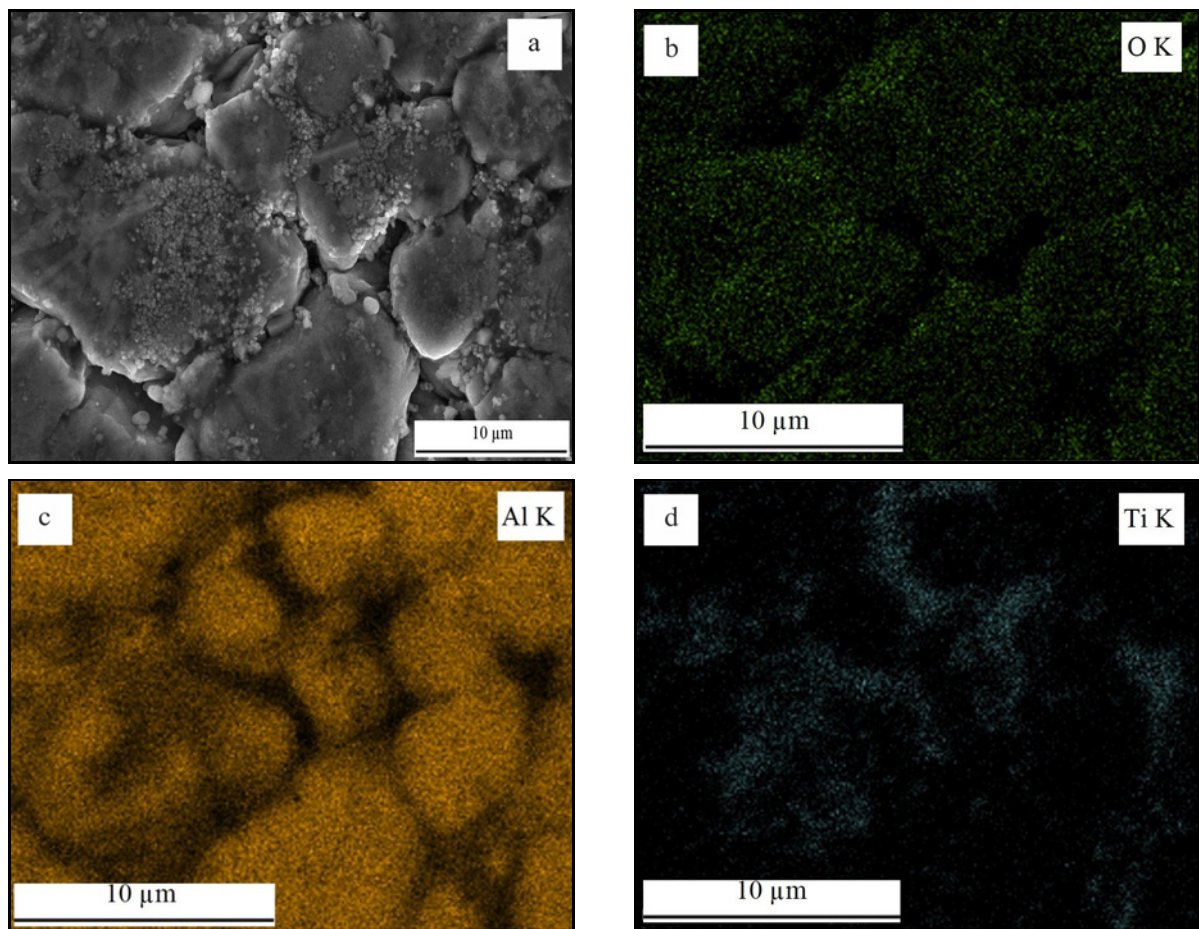
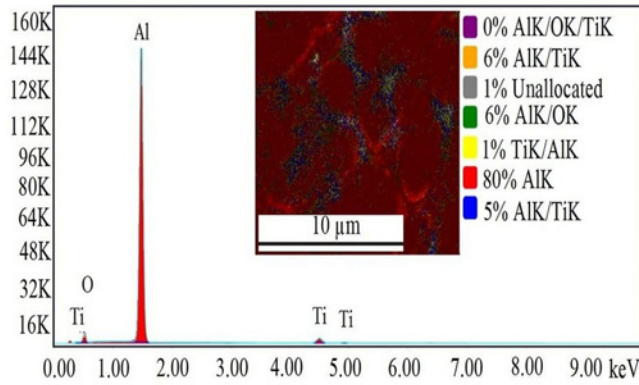


Fig. 3. SEM image of synthesized Al-20 wt.%  $\text{Al}_2\text{O}_3$ - $\text{TiO}_2$  composite (a) and EDS mapping of titanium (b), aluminum (c), and oxygen (d).



Element	Sum Spectrum		AlK/OK/TiK		AlK/TiK		Unallocated	
	Weight	Atomic	Weight	Atomic	Weight	Atomic	Weight	Atomic
	%	%	%	%	%	%	%	%
OK	4.65	7.83	29.24	47.15	7.14	12.73	11.88	23.01
AlK	88.03	88.04	35.30	33.75	69.14	73.14	39.86	45.77
TiK	7.32	4.13	35.46	19.10	23.72	14.13	48.26	31.22

Element	AlK/OK		TiK/AlK		AlK		AlK/TiK	
	Weight	Atomic	Weight	Atomic	Weight	Atomic	Weight	Atomic
	%	%	%	%	%	%	%	%
OK	19.14	29.62	7.11	16.06	3.35	5.57	5.08	10.24
AlK	71.39	65.49	23.66	31.69	94.25	93.09	49.30	59.00
TiK	9.46	4.89	69.24	52.25	2.40	1.34	45.62	30.76

Fig. 4. EDX spectrum and elemental mapping of Al-20 wt.% Al<sub>2</sub>O<sub>3</sub>-TiO<sub>2</sub> composite.

cantly impact the microstructure and properties of the metal matrix composites. Higher weight percentages of Al<sub>2</sub>O<sub>3</sub>-TiO<sub>2</sub> powder result in a more refined structure. This is due to the alumina and titanium oxide particles acting as barriers to the movement of grain boundaries, thus delaying grain growth [21]. Figure 2 shows that aluminum condensed during the sintering, and Al<sub>2</sub>O<sub>3</sub> and TiO<sub>2</sub> powder were undamaged since the melting temperature of Al<sub>2</sub>O<sub>3</sub>-TiO<sub>2</sub> powder is much higher than that of aluminum. Since the sintering process is carried out at a low temperature of 800 °C, some TiO<sub>2</sub> and Al<sub>2</sub>O<sub>3</sub> particles have remained unreacted. Besides, the composite samples have no sintering defects or cracks. Some large aluminum particles are slightly flattened, although the milling conditions were relatively mild, and cold welding did not occur.

SEM image and corresponding EDS mapping analysis of the composite powders are given in Figs. 3 and 4. These figures indicate the spectrum of Al/Al<sub>2</sub>O<sub>3</sub>-TiO<sub>2</sub> composite with peaks of aluminum and titanium, and elemental mapping confirms the presence of oxygen, aluminum, and titanium. The formation of other phases such as Al<sub>5</sub>Ti<sub>2</sub> is not distinguished in EDS.

Density measurement was carried on the Al/Al<sub>2</sub>O<sub>3</sub>-TiO<sub>2</sub> composites with different amounts of Al<sub>2</sub>O<sub>3</sub>-TiO<sub>2</sub> reinforcement. First, density was evaluated theoretically subject to the concept rule of mixtures. Archimedes' principle was used for calculating the experimental density of Al/Al<sub>2</sub>O<sub>3</sub>-TiO<sub>2</sub> MMC<sub>s</sub>, wherein the test samples were weighed up in air and fluid of known density (water in the current investigation).

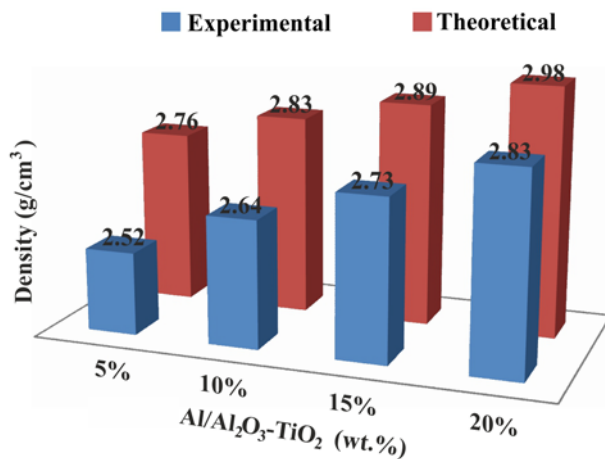


Fig. 5. Density (theoretical and experimental) values for different compositions of Al/Al<sub>2</sub>O<sub>3</sub>-TiO<sub>2</sub>.

Figure 5 presents the density (theoretical and experimental) values for different compositions of Al/Al<sub>2</sub>O<sub>3</sub>-TiO<sub>2</sub>. It can be stated based on the studies in the literature that Al<sub>2</sub>O<sub>3</sub> and TiO<sub>2</sub> reinforcements have lower density due to the previously indicated cluster formation during pressing and the need for extra pressure to enable softer metal particles for filling the pores between hard ceramic particles [23]. It can be stated based on Fig. 5 that both theoretical and experimental densities are in good agreement with each other, thus affirming the suitability powder metallurgy technique.

### 3.2. Mechanical characterization

Vickers hardness values of the sintered pure Al and Al/Al<sub>2</sub>O<sub>3</sub>-TiO<sub>2</sub> composite samples were calculated using at least five successive indentations for each sample by a Duroline-M Hardness Tester under a load of 1 kg for 15 s.

Vickers hardness for pure aluminum (Al) and the variation of Vickers hardness for Al/Al<sub>2</sub>O<sub>3</sub>-TiO<sub>2</sub> composites are shown in Fig. 6. It has also been noted that when wt.% of Al<sub>2</sub>O<sub>3</sub>-TiO<sub>2</sub> increases up to 10 wt.%, there is a slight increase in hardness value of Al/Al<sub>2</sub>O<sub>3</sub>-TiO<sub>2</sub> composite. This low hardness value is due to the near-uniform dispersion of reinforcement in the metal matrix phase and the cluster formation, which leads to porosity (Fig. 2). It can be seen that the hardness of Al/Al<sub>2</sub>O<sub>3</sub>-TiO<sub>2</sub> composite increases with an increase in the number of Al<sub>2</sub>O<sub>3</sub>-TiO<sub>2</sub> particles, maximum hardness was 56 HV, and it was due to the sample containing 20 wt.% of Al<sub>2</sub>O<sub>3</sub>-TiO<sub>2</sub> particles. This may be related to particles hindering matrix dislocation movement in the composite, thus leading to increased strength and hardness. Maity et al. [15] suggested that the presence of alumina particles can

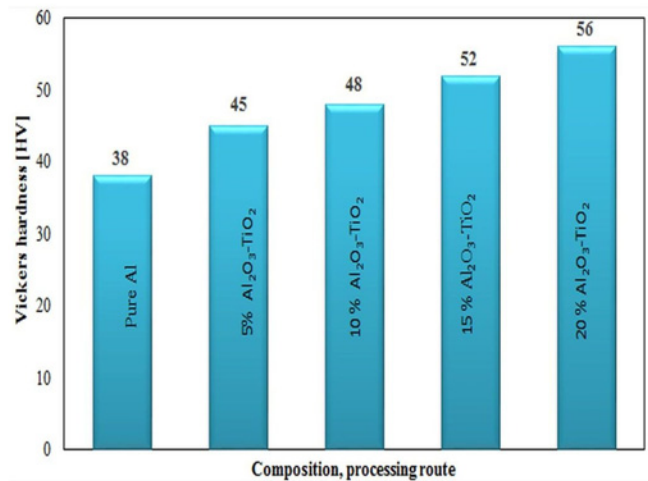


Fig. 6. Variation of Vickers hardness with different wt.% of Al<sub>2</sub>O<sub>3</sub>-TiO<sub>2</sub>.

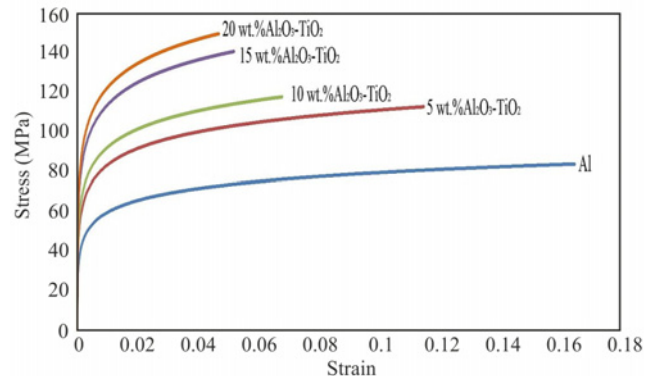


Fig. 7. Stress-strain curve of Al and Al/Al<sub>2</sub>O<sub>3</sub>-TiO<sub>2</sub> composite with different wt.% of Al<sub>2</sub>O<sub>3</sub>-TiO<sub>2</sub>.

increase the hardness of the Al alloy. Sheelvant et al. [23] have stated that reinforcing particles play an important role by sharing a main part of the contact load and support contact stresses for preventing plastic deformation, subsequently increasing the hardness of the composite. Das et al. [25] reported that the hardness of aluminum-based composites increased with increasing weight fraction reinforcements. With the increase in reinforcement weight content, the reinforcement-to-matrix ratio becomes richer, which provides increased hardness to the composite.

Figure 7 shows the tensile stress-strain curves for Al and Al/Al<sub>2</sub>O<sub>3</sub>-TiO<sub>2</sub> composites with 5, 10, 15, and 20 wt.% of alumina-titanium oxide. Adding Al<sub>2</sub>O<sub>3</sub> and TiO<sub>2</sub> reinforcing particles increases the tensile strength of aluminum matrix composite and keeps growing due to dispersion hardening. The composite strength is increased further by enhancing the bonding or relationship of liquid aluminum with Al<sub>2</sub>O<sub>3</sub> and TiO<sub>2</sub> particles. Tensile strength increased significantly

Table 2. Mechanical properties of various Al-MMC<sub>s</sub> composites

Reinforcement materials	Sintering temperature (°C)	Hardness	Strength $\sigma$ (MPa)	UTS (MPa)	References
Al/Fly ash, Al/aloe, and Al	720, stir casting method	28.2 and 33.8 BHN	53.36 and 62.97 (yield strength)	104.21 and 119.83	[2]
7075Al/TiB <sub>2</sub>	LMD process	1.97 GPA nanohardness	734 (comp. strength)	–	[3]
Al/Fe-based metallic glass	450/640 MPa via hot pressing	–	218 (yield strength)	374	[10]
Al/Al <sub>2</sub> O <sub>3</sub>	620 (sintered) 420 (extruded) 350 (annealed)	45.6 HRC (%1) 68.4 HRC (%7)	$\cong$ 130 (%1) $\cong$ 180 (%7) (yield strength)	–	[21]
TiB <sub>2</sub>	650, muffle furnace	$\cong$ 70 HV (%5)	–	–	[23]
Al/graphene	1400	57 HV	–	$\sim$ 120	[27]
Al/TiO <sub>2</sub>	700, stir casting method	104.6 BHN (%2), 124 BHN (%8)	–	$\cong$ 175 (%2), and $\cong$ 225 (% 8) tensile strength	[28]
Al/VC	600 (conventional sintering) 600 (microwave sintering) 450 (SPS)	232 $\pm$ 16 HV	295 (bending strength)	–	[29]

following the addition of 20 wt.% Al<sub>2</sub>O<sub>3</sub>-TiO<sub>2</sub>. A comparison was made between the mechanical properties of the composites obtained and those found from the related literature for dense Al/Al<sub>2</sub>O<sub>3</sub>-TiO<sub>2</sub> materials obtained through different processes (Table 2). This finding is in good agreement with previously published results [3, 8, 12, 21, 23–25]. Also, the reasons for lower values of hardness and tensile strength can be explained as follows:

The micrograph of some clusters in the Al matrix and porosity due to cluster formation indicates that the TiO<sub>2</sub> and Al<sub>2</sub>O<sub>3</sub> particles are surrounded by aluminum particles. This is related to the near-uniform dispersion of reinforcement in the metal matrix phase or the tendency of smaller particles to form cluster pressing, which overall contributes to increased material porosity and poor mechanical properties. Also, the lack of interfacial strength, partial wetting of particles, and the presence of constituent particles at the interface adversely affect its mechanical properties [15, 21].

Figure 7 shows that the higher the weight per-

centage of reinforcements in the matrix, the lower the toughness value is. This is due to obstacles to the motion of dislocation. Micron-sized particles are generally used for enhancing the metal tensile properties [25]. However, increasing ceramic reinforcement weight fractions lead to a significant decrease in the ductility of the composite.

It was observed that satisfactory results obtained mechanical properties (Figs. 6 and 7) of Al/Al<sub>2</sub>O<sub>3</sub>-TiO<sub>2</sub> composites produced via powder metallurgy specimens sintered at 800°C compared with those of the samples from similar studies in the literature (Table 2). The values we have achieved are close to those of similar composite materials studied in the literature.

Ghasali et al. [24] demonstrated that the formation of Al<sub>3</sub>Ti phases positively impacts the final mechanical properties of the aluminum matrix composite. Milman et al. [26] pointed out that Al<sub>3</sub>Ti compounds act as an useful reinforcement for aluminum alloys due to significant properties such as low density, high hardness, good high-temperature properties. Based on

phase analysis, it seems that a partial reaction occurs between Al and TiO<sub>2</sub> resulting in the formation of a small amount of Al<sub>5</sub>Ti<sub>2</sub>. Hence, the previously mentioned phase is considered to have the same effect as the Al<sub>3</sub>Ti phase.

#### 4. Conclusions

Al/Al<sub>2</sub>O<sub>3</sub>-TiO<sub>2</sub> composite samples used in the present study were fabricated with 5–20 wt.% of Al<sub>2</sub>O<sub>3</sub>-TiO<sub>2</sub> through milling, compacting, and sintering processes. Afterward, the structural (phase composition, microstructure, relative density), mechanical (tensile strength, hardness) properties of the composites were characterized. Aluminum matrix composite reinforced with alumina-titanium oxide (Al<sub>2</sub>O<sub>3</sub>-TiO<sub>2</sub>) was produced successfully during the current study by implementing powder metallurgy processing methods. The following conclusions were achieved:

- The diffraction peaks of Al, Al<sub>2</sub>O<sub>3</sub>, and TiO<sub>2</sub> phases were observed. The Al phase in the XRD patterns was represented by sharp peaks, and minor peaks indicated the presence of Al<sub>2</sub>O<sub>3</sub> and TiO<sub>2</sub> particles. The XRD results were also in accordance with the EDS results, which attests to the fabrication of phase pure different ceramic-reinforced Al-composites.

- The densities of the developed composite were in accordance with the theoretical values and displayed a near-uniform distribution of reinforcement particles. Samples with 20 wt.% of Al<sub>2</sub>O<sub>3</sub>-TiO<sub>2</sub> particles had a higher relative density of Al/Al<sub>2</sub>O<sub>3</sub>-TiO<sub>2</sub> composite. The highest relative density of 96 % was observed in specimens sintered at 800 °C.

- The tensile strength of composites at room temperature increases along with an increase in the Al<sub>2</sub>O<sub>3</sub>-TiO<sub>2</sub> composite powder's weight fraction from 5 to 20 wt.% in the Al matrix. Low inherent ductility of the ceramic particles used as reinforcement resulted in low ductility in the produced Al/Al<sub>2</sub>O<sub>3</sub>-TiO<sub>2</sub> composites compared to pure Al. Minimum and maximum tensile strength values for the composite samples were observed as 84 and 150 MPa, respectively. The low porosity level and the good distribution of ceramic particulates led to a good enhancement in tensile strength.

- The weight ratio of reinforcement-to-matrix increased further with increased reinforcement content resulting in increased hardness in the composite.

- Microstructure characterization and SEM micrographs of the composites revealed a fairly near-uniform distribution of Al<sub>2</sub>O<sub>3</sub> and TiO<sub>2</sub> particulates. Some unreacted TiO<sub>2</sub> clusters and discrete Al<sub>2</sub>O<sub>3</sub> particles were observed in the matrix.

#### References

- [1] P. S. Bains, S. S. Sidhu, H. S. Payal, Fabrication and machining of metal matrix composites: A review, *Mater. Manuf. Processes* 31 (2016) 553–573. [doi:10.1080/10426914.2015.1025976](https://doi.org/10.1080/10426914.2015.1025976)
- [2] C. H. Gireesh, K. G. Durga Prasad, K. Ramji, P. V. Vinay, Mechanical characterization of aluminium metal matrix composite reinforced with aloe vera powder, *Materials Today: Proceedings* 5 (2018) 3289–3297. [doi:10.1016/j.matpr.2017.11.571](https://doi.org/10.1016/j.matpr.2017.11.571)
- [3] B. Jiang, L. Zhenglong, C. Xi, L. Peng, L. Nannan, C. Yanbin, Microstructure and mechanical properties of TiB<sub>2</sub>-reinforced 7075 aluminum matrix composites fabricated by laser melting deposition, *Ceramics International* 45 (2019) 5680–5692. [doi:10.1016/j.ceramint.2018.12.033](https://doi.org/10.1016/j.ceramint.2018.12.033)
- [4] K. D. Salman, Comparison of the physical and mechanical properties of composite materials (Al/SiC and Al/B<sub>4</sub>C) produced by powder technology, *Journal of Eng.* 23 (2017) 85–96.
- [5] N. Muralidharan, K. Chockalingam, I. Dinaharan, K. Kalaiselvan, Microstructure and mechanical behavior of AA2024 aluminum matrix composites reinforced with in situ synthesized ZrB<sub>2</sub> particles, *J. Alloys Compd.* 735 (2018) 2167–2174. [doi:10.1016/j.jallcom.2017.11.371](https://doi.org/10.1016/j.jallcom.2017.11.371)
- [6] J. David R. Selvam, I. Dinaharan, V. Philip, S. Mashinini, Microstructure and mechanical characterization of in situ synthesized AA6061/(TiB<sub>2</sub>+Al<sub>2</sub>O<sub>3</sub>) hybrid aluminum matrix composites, *J. Alloys Compd.* 740 (2018) 529–535. [doi:10.1016/j.jallcom.2018.01.016](https://doi.org/10.1016/j.jallcom.2018.01.016)
- [7] S. K. Josyula, S. K. R. Narala, Machinability enhancement of stir cast Al-TiC<sub>p</sub> composites under cryogenic condition, *Mater. Manuf. Processes* 32 (2017) 1764–1774. [doi:10.1080/10426914.2017.1303151](https://doi.org/10.1080/10426914.2017.1303151)
- [8] S. Mohit, S. Raj, Fabrication of aluminum matrix composites by stir casting technique and stirring process parameters optimization, *Advanced Casting Technologies* (2018) 112–125. [doi:10.5772/intechopen.73485](https://doi.org/10.5772/intechopen.73485)
- [9] S. Sivasankaran, K. Sivaprasad, R. Narayanasamy, P. V. Satyanarayana, X-ray peak broadening analysis of AA 6061<sub>100-x-x</sub> wt.% Al<sub>2</sub>O<sub>3</sub> nanocomposite prepared by mechanical alloying, *Material Characterization* 62 (2011) 661–672. [doi:10.1016/j.matchar.2011.04.017](https://doi.org/10.1016/j.matchar.2011.04.017)
- [10] T. He, T. Lu, N. Ciftci, H. Tan, V. Uhlenwinkel, K. Nielsch, S. Scudino, Mechanical properties and tribological behavior of aluminum matrix composites reinforced with Fe-based metallic glass particles: Influence of particle size, *Powder Technology* 361 (2020) 512–519. [doi:10.1016/j.powtec.2019.11.088](https://doi.org/10.1016/j.powtec.2019.11.088)
- [11] E. Ervina, N. Siti, A. Mohd, M. Al Bakri, Fabrication method of aluminum matrix composite (AMCs): A review, *Key Engineering Materials* 700 (2016) 102–110. [doi:10.4028/www.scientific.net/KEM.700.102](https://doi.org/10.4028/www.scientific.net/KEM.700.102)
- [12] V. K. Pandey, B. P. Patel, S. Guruprasad, Role of ceramic particulate reinforcements on mechanical properties and fracture behavior of aluminum-based composites, *Materials Science & Engineering A* 745 (2019) 252–264. [doi:10.1016/j.msea.2018.12.030](https://doi.org/10.1016/j.msea.2018.12.030)
- [13] P. Gudlur, A. Forness, J. Lentz, M. Radovic, A. Muliana, Thermal and mechanical properties of Al/Al<sub>2</sub>O<sub>3</sub>

- composites at elevated temperatures, *Materials Science and Engineering A* 531 (2012) 18–27. [doi:10.1016/j.msea.2011.10.001](https://doi.org/10.1016/j.msea.2011.10.001)
- [14] T. Theivasanthi, A. Marimuthu, Titanium dioxide (TiO<sub>2</sub>) nanoparticles XRD analyses: An insight, *Chemical Physics* (2013) arXiv:1307.1091. (<http://arxiv.org/abs/1307.1091>)
- [15] P. C. Maity, P. N. Chakraborty, S. C. Panigrahi, Processing and properties of Al-Al<sub>2</sub>O<sub>3</sub> (TiO<sub>2</sub>) in situ particle composite, *Journal of Materials Processing Technology* 53 (1995) 857–870. [doi:10.1016/0924-0136\(94\)01757-R](https://doi.org/10.1016/0924-0136(94)01757-R)
- [16] V. V. Vani, S. K. Chak, The effect of process parameters in aluminum metal matrix composites with powder metallurgy, *Manufacturing Rev.* 5 (2018) 7. [doi:10.1051/mfreview/2018001](https://doi.org/10.1051/mfreview/2018001)
- [17] K. Das, P. Choudhury, S. Das, The Al-O-Ti (aluminum-oxygen-titanium) system, *Journal of Phase Equilibria* 23 (2002) 525–536. [doi:10.1361/105497102770331271](https://doi.org/10.1361/105497102770331271)
- [18] A. E. Nassar, E. E. Nassar, Properties of aluminum matrix nano composites prepared by powder metallurgy processing, *Journal of King Saud University-Engineering Sciences* 29 (2017) 295–299. [doi:10.1016/j.jksues.2015.11.001](https://doi.org/10.1016/j.jksues.2015.11.001)
- [19] M. Rahimian, N. Ehsani, N. Parvin, H. R. Baharvandi, The effect of particle size, sintering temperature and sintering time on the properties of Al-Al<sub>2</sub>O<sub>3</sub> composites, made by powder metallurgy, *J. Mater. Proc. Technology* 209 (2009) 5387–93. [doi:10.1016/j.jmatprotec.2009.04.007](https://doi.org/10.1016/j.jmatprotec.2009.04.007)
- [20] A. Olszówka-Myalska, J. Szala, J. Cwajna, Characterization of reinforcement distribution in Al/(Al<sub>2</sub>O<sub>3</sub>)<sub>p</sub> composites obtained from composite powder, *J. Materials Characterization* 46 (2001) 189–195. [doi:10.1016/S1044-5803\(01\)00123-1](https://doi.org/10.1016/S1044-5803(01)00123-1)
- [21] Y. C. Kang, S. L. Chan, Tensile properties of nanometric Al<sub>2</sub>O<sub>3</sub> particulate-reinforced aluminum matrix composites, *Materials Chemistry and Physics* 85 (2004) 438–443. [doi:10.1016/j.matchemphys.2004.02.002](https://doi.org/10.1016/j.matchemphys.2004.02.002)
- [22] M. Šnajdar-Musa, Z. Schauerl, ECAP – New consolidation method for production of aluminum matrix composites with ceramic reinforcement, *Processing and Application of Ceramics* 7 (2013) 63–68. [doi:10.2298/PAC1302063S](https://doi.org/10.2298/PAC1302063S)
- [23] A. Sheelwant, S. K. Reddy Narala, P. Shailesh, Synthesis and tribological evaluation of aluminum-titanium diboride (Al-TiB<sub>2</sub>) metal matrix composite, *Materials Today: Proceedings* 28 (2020) 651–658. [doi:10.1016/j.matpr.2019.12.237](https://doi.org/10.1016/j.matpr.2019.12.237)
- [24] E. Ghasali, M. Alizadeh, T. Ebadzadeh, TiO<sub>2</sub> ceramic particles-reinforced aluminum matrix composite prepared by conventional, microwave, and spark plasma sintering, *Journal of Composite Materials* 52 (2017) 2609. [doi:10.1177/0021998317751283](https://doi.org/10.1177/0021998317751283)
- [25] D. K. Das, P. C. Mishra, S. Singh, R. K. Thakur, Properties of ceramic-reinforced aluminium matrix composites – A review, *Int. J. Mech. Mater. Eng.* 9 (2014) 12. [doi:10.1186/s40712-014-0012-9](https://doi.org/10.1186/s40712-014-0012-9)
- [26] Y. V. Milman, D. B. Miracle, S. I. Chugunova, I. V. Voskoboinik, N. P. Korzhova, T. N. Legkaya, Y. N. Podrezov, Mechanical behavior of Al<sub>3</sub>Ti intermetallic and L12 phases on its basis, *Intermetallics* 9 (2001) 839–845. [doi:10.1016/S0966-9795\(01\)00073-5](https://doi.org/10.1016/S0966-9795(01)00073-5)
- [27] M. C. Senel, M. Gurbuz, Effect of graphene content on tensile strength and microstructure of aluminum matrix composites, *Universal Journal of Materials Science* 6 (2018) 79–84. [doi:10.13189/ujms.2018.060301](https://doi.org/10.13189/ujms.2018.060301)
- [28] S. Siddesha, T. D. Jagannath, T. R. Punith, N. S. Rakshith, Effects of fabrication of aluminium 2024/TiO<sub>2</sub> metal matrix composite, *International J. of Innovative Res. and Dev.* 5 (2016) 174–177. [doi:10.1016/j.matpr.2018.02.170](https://doi.org/10.1016/j.matpr.2018.02.170)
- [29] E. Ghasali, A. H. Pakseresht, M. Alizadeh, T. Ebadzadeh, Vanadium carbide reinforced aluminum matrix composite prepared by conventional, microwave and spark plasma sintering, *J. Alloys Comp.* 688 (2016) 527–533. [doi:10.1016/j.jallcom.2016.07.063](https://doi.org/10.1016/j.jallcom.2016.07.063)